Biomedical Sciences
2016; 2(1): 1-10
http://www.sciencepublishinggroup.com/j/bs
doi: 10.11648/j.bs.20160201.11

Three-Dimensional Structure of RNA-Binding Protein TLS Co-Crystallized with Biotinylated Isoxazole

Riki Kurokawa[1, *], Toshikazu Bando[2]

[1]Division of Gene Structure and Function, Research Center for Genomic Medicine, Saitama Medical University, Saitama, Japan

[2]Department of Chemistry, Graduate School of Science, Kyoto University, Kyoto, Japan

Email address:

rkurokaw@saitama-med.ac.jp (R. Kurokawa)

[*]Corresponding author

To cite this article:

Riki Kurokawa, Toshikazu Bando. Three-Dimensional Structure of RNA-Binding Protein TLS Co-Crystallized with Biotinylated Isoxazole. *Biomedical Sciences.* Vol. 2, No. 1, 2016, pp. 1-10. doi: 10.11648/j.bs.20160201.11

Received: April 7, 2016; **Accepted**: April 13, 2016; **Published**: June 3, 2016

Abstract: RNA-binding protein TLS with specific mutations forms insoluble precipitates in motor neurons causing neuronal degenerative diseases like amyotrophic lateral sclerosis (ALS), and frontotemporal dementia. TLS at high concentration around 10 mg/ml is prone to be precipitated even without any mutation. The mutation on TLS is supposed to induce more precipitation than the wild type with uncovered molecular mechanism. Specific protein precipitation is one of major causes for the neuronal diseases like the Alzheimer disease with amyloid formations. Identification of a trigger of the precipitation formation is a key event at developing the therapeutics against these diseases. Screening candidate compounds from a chemical library to stimulate mouse embryonic stem cells into cardiomyocytes identified isoxazole, its relative compounds containing the COX-2 inhibitor and β lactamase-resistant antibiotics. Its derivative, biotinylated isoxazole (b-isox), was serendipitously found to be precipitated with divergent RNA-binding proteins through their low complexity domains. The b-isox precipitation of RNA-binding proteins should be a model system for formation of insoluble precipitates at neuronal degenerative diseases. We confirmed the precipitation of TLS with b-isox and analyzed the co-crystal formation. In silico analysis presents a model of crystallization of b-isox forming the β strand structure with wavy repetitive valleys. The valleys of the β sheet capture the unstructured LC domains of TLS and force them into also β strand shapes. This model sheds light on flexible feature of the LC domain that well fits the valleys of the b-isox crystals. This should be one major reason why various LC domains are involves in formation of insoluble precipitates, suggesting molecular mechanism for neurodegenerative disorders.

Keywords: TLS, FUS, Biotinylated Isoxazole, Low Complexity Domain, Amyotrophic Lateral Sclerosis

1. Introduction

Physiology or Medicine of RNA has been getting more impact on modern biology extending the previous views for the RNA metabolism that is just oriented to a step of gene expression at the context of the Central Dogma [1-9]. The extensive works on transcriptome inspections of the human genome-derived RNAs enlighten huge numbers of RNAs transcribed from noncoding DNA regions [10-12]. Most of the unidentified transcripts are supposed to be unannotated long noncoding RNAs (lncRNAs) which biological activity remains mostly undescribed[13]. These lncRNAs are transcribed from highly divergent sequences of the human genome like retrotransposons LINE/SINE and also numerous pseudogenes [4, 14-17]. Thus, their sequences are in full diversity and unlikely to have a common molecular mechanism behind of their biological activity. We have, however, noticed that most of RNAs are supposed to have its own RNA binding protein partner in living cells[18]. Then, we have set RNA-binding proteins as a criterion for classification of biological activities for each lncRNA. For this end, analysis of a model system of RNA binding is employed to initiate this project.

We pick RNA-binding protein TLS as a model molecule to be elucidated [19]. At this manuscript, we have performed biochemical analysis of TLS related to a small molecular weight chemical compound, biotinylated isoxazole (b-isox). B-isox has unique nature specifically precipitating certain species of RNA-binding proteins [20, 21]. This sort of the precipitation is one of crucial event at the cause of many

neuronal degenerative diseases like ALS. Revealing diseases of RNA-binding proteins will bring unprecedented insight into biology of their physiological ligands, lncRNAs [22-26]. Therefore, we describe experimental and in silico analysis of chemical nature of b-isox precipitation with TLS extensively. This presents a promise to new pathway of investigation in lncRNA biology.

We, then, perform the in silico analysis of three-dimensional structure of b-isox crystals with TLS in order to elucidate interaction of these molecules. We have constructed a multilayer model of the crystal of b-isox based upon the Cambridge Structural Database. At the multilayer model, the b-isox molecules form an antiparallel structures, while, in a layer they make hydrogen bonds with neighboring molecules and between other layers, they form hydrogen bonds through the biotin moiety of the molecules.

In a layer, the b-isox molecules mimic β strand-like bonds through the amide and the carbonyl groups. At our model of the complex of the β strand of the polypeptides with the crystals of b-isox molecules, the main chains of the β strands could form the β strand-like hydrogen bonds with the b-isox molecules. The main chains of the peptides are supposed to bind to the b-isox molecules upon forming the β strand-like hydrogen bonds with them.

The LC domain of TLS contains many tyrosine (Y), glutamine (Q), and serine residues(S). These three side chains are likely to form hydrogen bonds through carbonyl groups to the biotin moiety of the b-isox. These Y, Q, and S of the LC domain should enhance affinity of TLS, to the b-isox significantly. The LC domain of TLS represents a natively unfolded region that does not form any specific secondary structure [18]. The LC domain without any hydrogen bond inside is suitable to form the β strand-like hydrogen bonds with the b-isox molecules. Additionally, the hydrogen bond formation of Y, Q, and S of the LC domain with the b-isox molecules induces their binding to the b-isox molecules.

During development of the b-isox crystals, the Y, Q, and S of the LC domain of TLS could form the β strand-like hydrogen bonds of the main chain, and the hydrogen bonds of the side chains to the crystals, incorporated into the b-isox crystal structures. The Y, Q, and S of the LC domain of TLS are supposed to bind to multiple points of surfaces of the b-isox crystals and grow up to the large complexes.

2. Materials and Methods

2.1. Materials

Screening the chemical library to obtain chemical compounds to induce mouse embryonic stem cells into myocardial cell lineages presented a chemical compound, isoxazole [27]. Biotinylated isoxazole (b-isox), 6-(((5-(2-Thienyl) -1,2-oxazol-3-yl)carbonyl)amino)hexyl,5-(2-oxohexahydro-1 H-thieno[3,4-d]imidazol-4-yl)pentanoate (biotin-isoxazole; b-isox) was produced following the protocols [20]. Chemical Synthesis of b-isox was performed following the previous publication [20]. HeLa cell nuclear extract was prepared as previously described protocol [19, 28]

2.2. Protein Analysis

SDS-polyacrylamide gel electrophoresis was performed with 10% gels following coomassie brilliant blue staining [18]. Western blotting was done with anti-TLS monoclonal antibody from the BD bioscience, 611385 with the dilution ratio 1:2000 using standard protocol shown previously [18].

2.3. In Silico Analysis of the LC Domains and the Crystals of b-isox

The structural coordinate data of the b-isox crystal (Accession number 873064) [20] was obtained from Cambridge Structural Database: CSD;

http://www.ccdc.cam.ac.uk.

A model of the main chains of the theoretical β strand structure was constructed with the parameters setting at the dihedral angles Φ and Ψ set at 120° using the software Swiss-Pdb viewer [29]. The β strand model was docked into the crystals of b-isox molecules by superimposing the β strand model on the b-isox molecules with Waals (The Altif laboratory, Inc.). Structural models of β strand with the side chain (Y, Q, and S) were built using Swiss-PdbViewer [29].

The side chain rotamers with no steric conflict and proper hydrogen bonds between the side chain of β strand structure and b-isox molecules were screened, and the energy minimization was performed to optimize the conformations [30]. The divergent conformations of the b-isox molecule were constructed with the chemical structural modeling software Marvin (ChemAxon, Budapest, Hungary).

We obtained the data of the b-isox crystal (Accession number 873064) from Cambridge Structural Database: CSD; http://www.ccdc.cam.ac.uk. CSD has been administrated with the Cambridge Crystallographic Data Center. The database contains data regarding crystals of organic chemical compounds and metalorganic chemical compounds. We obtained the crystal structural data consisting of its crystal lattice and atomic coordinate of asymmetry unit.

3. Results

3.1. Precipitation of TLS with b-isox at 4°C

We performed incubation of TLS with 100 μM b-isox at 4°C and obtained an immediate observation of flocculent and pure white precipitates at the tube. Analyzing the precipitates with a SDS-polyacrylamide gel electrophoresis presents hundreds of protein bands staining with coomassie brilliant blue (Fig. 1A). These bands are supposed to be proteins with the LC domain containing TLS [20]. The precipitates were warmed up to 37°C and disappeared (Fig. 1A). We executed a Western blot of the same precipitates with anti-TLS antibody and detected a specific band recognized by the antibody at the right molecular weight position of the gel (Fig.1B).

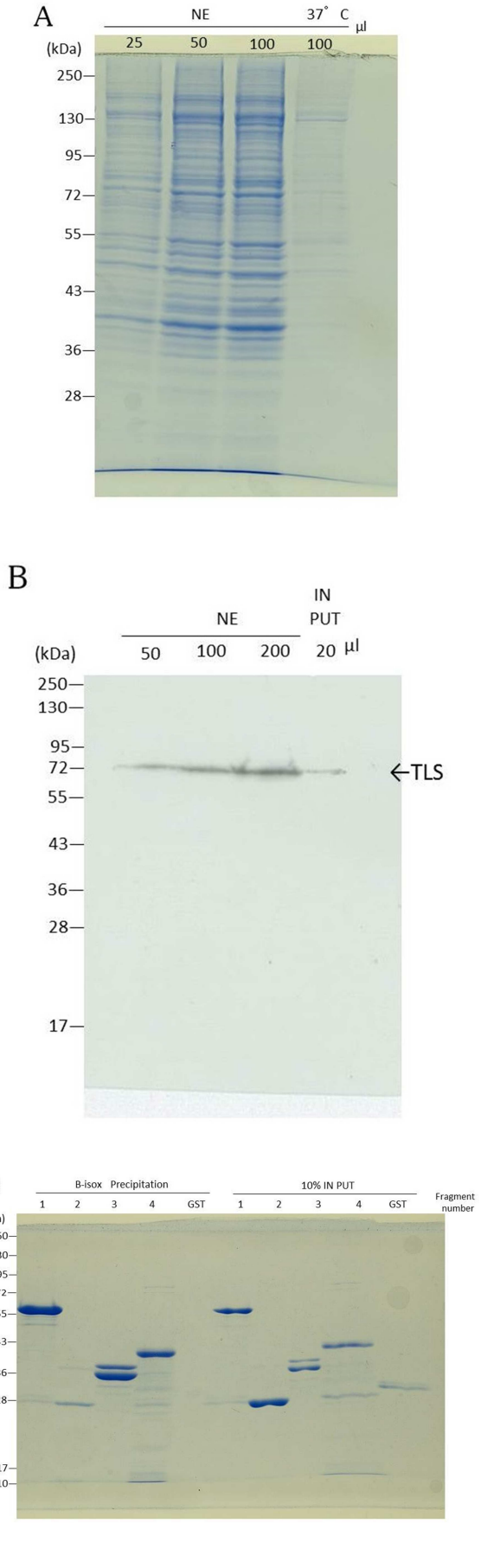

Figure 1. *Precipitation of TLS from HeLa cell nuclear extract with b-isox*

(A) SDS-PAGE shows the precipitated proteins with b-isox.
(B) Western blot shows the precipitation of TLS with b-isox.
(C) The mapping of target fragment of GST-TLS. Precipitation of GST-TLS fragments.
(D) The fragments of GST-TLS.
(E) Concentration dependency of the b-isox precipitation of TLS. The Western blotting of the samples shown was performed with the monoclonal antibody against TLS (1:2000).

A mapping experiment of target region at TLS has been executed with four fragments of GST-TLS (Fig.1C). It shows that the fragment 1, 3, and 4 of the GST-TLS are precipitated well with b-isox (Fig.1CD). The GST-TLS-1 contains the LC domain. The GST-TLS-3 has a prion domain. The prion domain has been reported to form pathological aggregates [31, 32]. The fragment 4 does not have any published target sequence of b-isox, but should contain unidentified preference motif there. The data present b-isox as a possible inducer for the prion disease related precipitations.

To eliminate whole TLS from the nuclear extract, we explored range of the concentration of b-isox. 100 μM of b-isox precipitate most of TLS in the nuclear extract, although there is still some amount of TLS left in the supernatant after the precipitation (Figure 1E). More than 250 μM b-isox completely removed TLS from the nuclear extract. Concentration-dependency of the b-isox precipitation of TLS is clearly shown.

3.2. Multilayer Model of b-isox

3.2.1. Biotinylated Isoxazole (b-isox)

Screening the chemical library to obtain chemical compounds to induce mouse embryonic stem cells into myocardial cell lineages presented a chemical compound, isoxazole[27]. The b-isox has a structure of a carbon chain connecting the isoxazole to the biotin moiety (Fig.2).

We obtained the data of the b-isox crystal (Accession number 873064) from the Cambridge Structural Database: CSD; http://www.ccdc.cam.ac.uk. CSD has been administrated with the Cambridge Crystallographic Data Center. The database contains data regarding crystals of organic chemical compounds and metalorganic chemical compounds. We obtained the crystal structural data consisting of its crystal lattice and atomic coordinate of asymmetry unit.

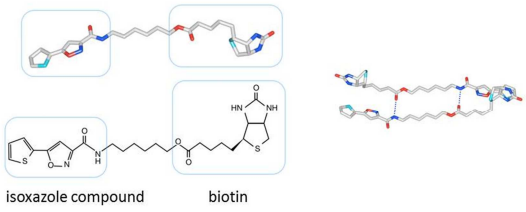

Figure 2. *B-isox molecule and its crystal structure.*

Molecular structure of b-isox (Left panel); The antiparallel conformation of the b-isox molecules (Right panel).

3.2.2. The Multilayer Model of b-isox

We construct a multilayer model of b-isox based upon the published data [20]. The data consists of the asymmetrical atomic coordinate of the crystal lattice of b-isox, obtained from CSD. It represents symmetrical crystal structures of b-isox (Fig.3A). In the crystal, the b-isox molecules are fully extended. There two molecules align as a position of an antiparallel orientation to form layers of molecules. The surface of the multilayered crystal forms a concavo-convex shape, a valley and mountain shape.

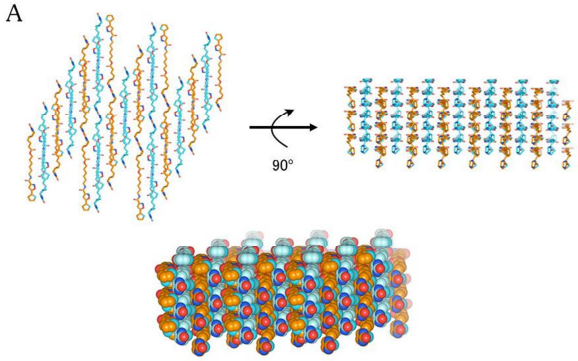

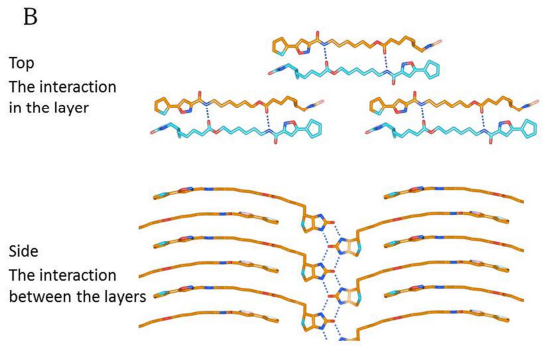

Figure 3. *Models for the b-isox crystal.*

(A) The top view of the model (Left panel); the side view (Right panel). The surface of the crystal forms concavo-convex shape (Bottom panel).

(B) The b-isox molecules just only at the same layer are shown. The adjacent two molecules form hydrogen bonds of the carbonyl group of the biotin moiety and of the amide group of the isoxazole moiety (Upper panel).

One row of the crystal is shown. The biotin moiety binds each other intimately (Lower panel).

3.2.3. Characteristic Structure of the b-isox Crystal

In the multilayer structure, the b-isox molecules interact inside of the layers and also between the layers (Fig.3AB). In the layers, two b-isox molecules aligned at the antiparallel orientation forms hydrogen bonds through the carbonyl groups of the biotin moiety and the amide groups of the isoxazole portion, each other. Between the layers, the nitrogen atoms and oxygen atom of the biotin molecules, forms hydrogen bonds, inducing into more stacked status (Fig.3B).

Comparing the aligned two b-isox molecules and the polypeptides aligned at the antiparallel orientation forming the β strands makes insight into similarity between the hydrogen bonds of the carbonyl groups and amide groups (Fig.4A). The calculated distance between two molecules of b-isox is 4.7 Å on average. This distance has nice agreement to the one between the β strands. The crystals of the b-isox could grow extendedly with forming hydrogen bonds that are insides of the layers of the β strands and between its biotin moieties.

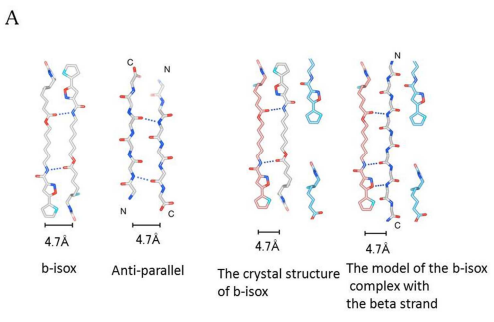

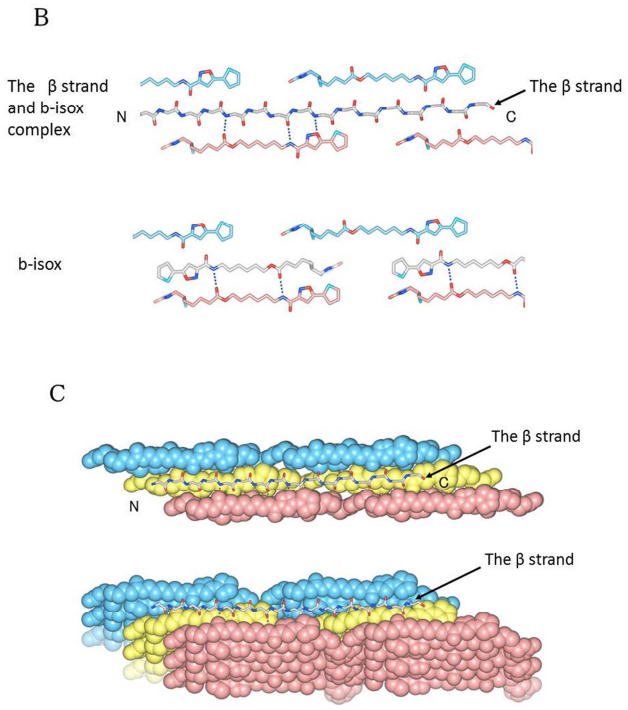

Figure 4. *Hydrogen bonds in the b-isox crystal.*

(A) Adjacent two b-isox molecules have an antiparallel conformation and hydrogen bonds. These two b-isox forms the β strand-like hydrogen bonds (Left panel). In the crystal, the hydrogen bonds between b-isox molecules, and the hydrogen bonds of the β strands are shown (Right panel).

(B) Binding of b-isox to the main chain. The b-isox model with the β strand (Upper panel); The b-isox crystal structure (Lower Panel).

(C) The model of the complex of b-isox and the main chain of the β strand Sticks; b-isox is shown as space filling format.

3.3. The Model of Binding of the LC Domain of TLS to the Crystal of b-isox

The LC domain of the N-terminal TLS represents disordered and naturally unfolded region [18]. We predicted how the polypeptides of the LC domain are incorporated into the crystal of b-isox forming the β strand structure. We build the model for the molecular events.

3.3.1. Binding of the Main Chains of the β Strand to b-isox

First of all, we build a model of the main chains of the theoretical β strand structure to deduce binding of the main chains of the β strand to b-isox. The model of the complex is designated to set the β strand in order to place the β strand to incorporate into the groove forming along to the skeletal structures of the b-isox molecules and to form hydrogen bonds between contiguous b-isox molecules inside of the layers of the b-isox crystal.

We build the main chain model of the β strand structure to make the glycine polypeptides with the parameters setting at the dihedral angles Φ and Ψ set at 120° using the software Pdb viewer. The software Waals (The Altif laboratory, Inc.) was employed to make the model by superimposing theβ strand model on the b-isox molecules and the b-isox and placing the β strand model into the crystals of b-isox molecules. The model shows that the polypeptide of the β strand fits between the adjacent b-isox molecules (light red and light blue) without any steric hindrance (Fig.4B; Fig. 5A,)[30]. The main chain of the β strand could form hydrogen bonds to adjacent b-isox molecules (light red) through the amide group and carbonyl group of the β strand like the crystal formation (Fig.4BC). Moreover, the main chain of the β strand could form hydrogen bond with the isoxazole moiety of the b-isox molecule. In the crystal, the b-isox molecules form the β strand-like hydrogen bonds. Replacing these b-isox molecules with the polypeptides of the β strand is confirmed to form the β strand-like structure with forming these hydrogen bonds. The main chain of the polypeptides could bind to the crystal of b-isox with the hydrogen bonds (Fig.4C).

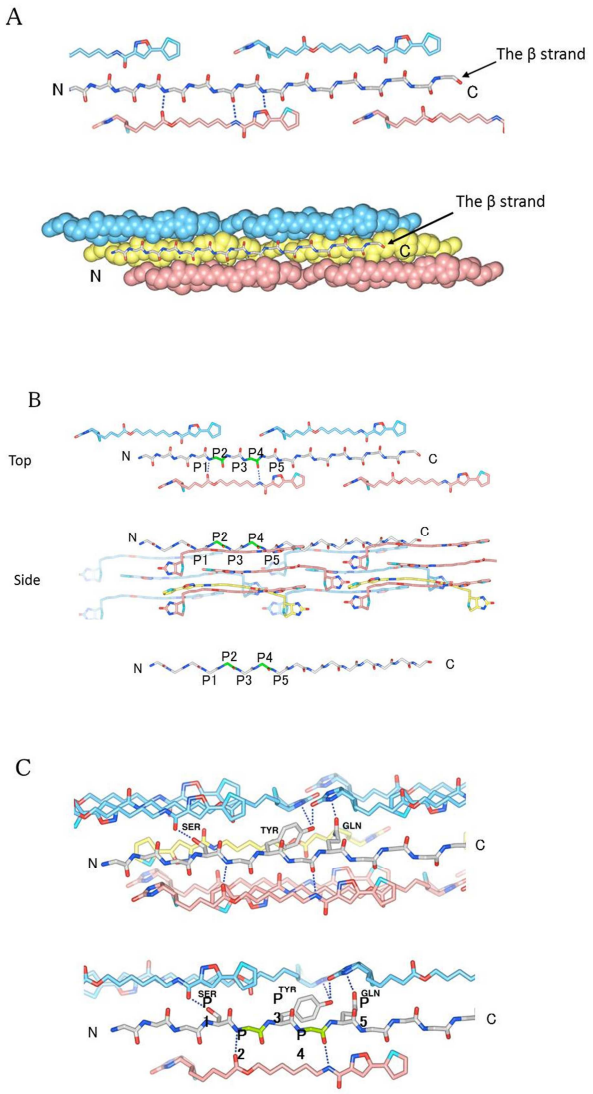

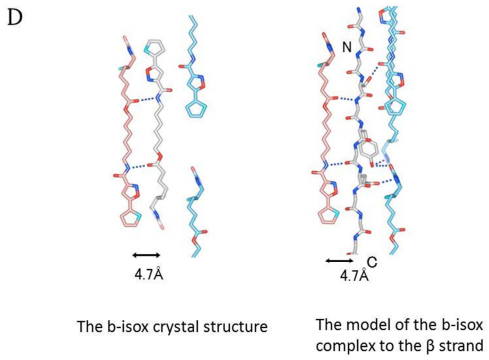

Figure 5. *The model of the complex between b-isox and the main chain of the β strand.*

(A) The model of the complex of b-isox to the main chain of the β strand
(B) Binding of b-isox to the side chain of the β strand. The amino acid residues that form the hydrogen bonds with the β strand are designated as P1, P2, P3, P4, and P5. The residues (P2 and P4) form the β strand-like hydrogen bonds shown as green. Side chains of P1, P3, and P5 face upward, while ones of P2 and P4 face downward.
(C) Binding of b-isox to the side chain of the β strand.
(D) Interaction of b-isox with the β strand (SGYGQ).

3.3.2. The Side Chain of the β Strand Interacts with b-isox

Next, we try to produce a model for real binding of TLS to the b-isox molecules and examine interaction of the side chain of the β strand to b-isox. The LC domain of TLS contains numerous Y, Q and S. We make a model of the complex in the case of the side chains of the β strand altered to Y, Q, and S, and test interaction of the side chains to b-isox.

At the model of the b-isox complex with the β strand, we set the amino acid residues positioned as P1, P2, P3, P4, and P5 of the hydrogen bonds of the β strand (Fig.5AB). The amino acid residues forming hydrogen bonds with the β strand are designated as P2 and P4 (green). The amino acid residue P2 binds the b-isox molecule by the amide group, while, the amino acid residue P4 binds the b-isox molecule by the carbonyl group. From the point of side view of the β strand, P1, P3, and P5 face downward, while, P2 and P4 face upward. The hydrogen bond formation of P2 and P4 (light red) of the polypeptide with the b-isox requires fitting of the side chains of P1, P3, and P5 inside without any steric hindrance, also favoring its interaction with b-isox.

Table 1. *The side chains of the β strand and interaction to b-isox.*

	P1	P3	P5
Tyr	—	hydrogen bond with biotin	—
Gln	hydrogen bond with carbonyl	hydrogen bond with carbonyl	hydrogen bond with biotin
Ser	hydrogen bond with carbonyl	—	hydrogen bond with biotin

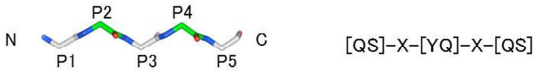

Then, P1, P3, and P5 are replaced with Y, Q, and S and incorporated into a model of the complex with b-isox (Fig.5CD). At the model, P1 could make a hydrogen bond with the side chains of Q and S, and the carbonyl groups of b-isox. P3 would make a hydrogen bond with the side chains of Y and the biotin moiety of b-isox, and its carbonyl group. P5 could have a hydrogen bond with Q, S, and the biotin moiety of b-isox.

The interaction of b-isox and the side chains of the β strand is summarized (Table 1). The side chains of P2 and P5 have no binding because of upward orientation of these residues. Given P1, P3, P5 as Q or S, Y or Q, Q or S, respectively, common motif should be as [QS]-X-[YQ]-X-[QS] (X: any amino acid residue without breaking the β strand). One example of the motif is the SGYGQ, shown (Fig.6ABC). At this consensus, two main chains of glycine form the β strand-like hydrogen bond with b-isox. The serine residue forms a hydrogen bond the carbonyl group of b-isox, while Y and Q form hydrogen bonds with the biotin moiety of b-isox. The hydrogen bond formation of these three side chains plays pivotal roles in crystallization of b-isox with the LC domain of TLS.

3.3.3. Binding of TLS to the b-isox Crystal

We explore molecular mechanisms of forming the insoluble precipitates of b-isox with TLS. Our model clearly shows that the LC domain of TLS is sliding into the valley of the b-isox crystals during their growing. The step of incorporation of TLS into the crystal requires the flexibility of the LC domain. This should be a major reason that the precipitates of b-isox contain vast amount of RNA-binding proteins having the LC domain [20]. Our biochemical analysis also indicates other portions of TLS other than the LC domain are precipitated with b-isox (Figure 1CD), suggesting other surfaces of TLS might be involved in the crystal formation. This should be pursued at the next chapter of the present project.

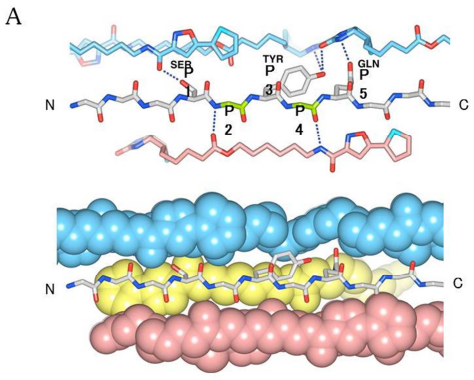

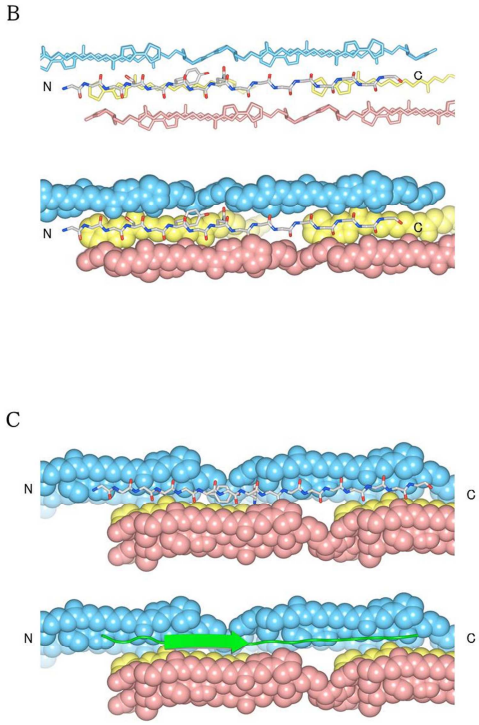

Figure 6. *(A)(B)(C) The model of the complex of b-isox to the β strand (SGYGQ) at the three independent conditions.*

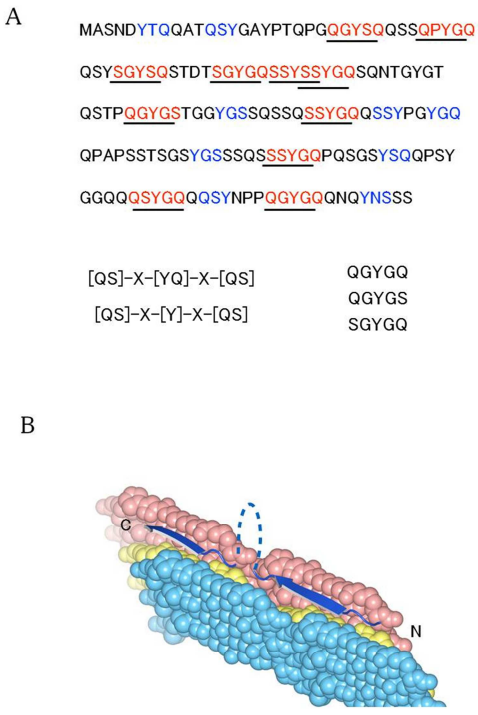

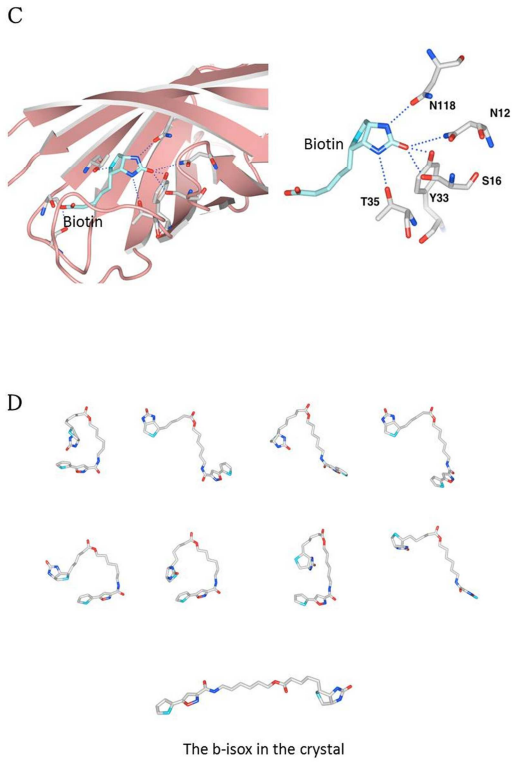

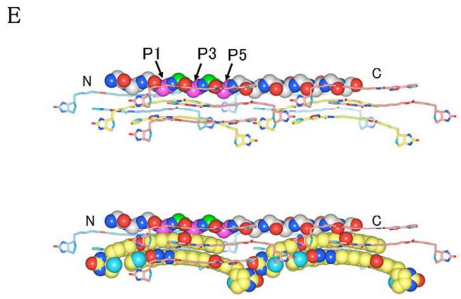

Figure 7. *The models of binding of b-isox to the LC domain of TLS.*

(A) Consensus motif QS-X-YQ-X-QS at the LC domain of TLS
(B) The model of binding of b-isox to the β strand.
(C) The binding of biotin to avidin (PDB ID: 2AVI) [33]. At the complex of biotin to avidin, the amino acid residues of avidin that are involved in binding to biotin are shown as Sticks. The side chains of Tyr 35, Thr35, and Asn118, form hydrogen bonds to b-isox. These hydrogen bonds of b-isox are the similar one that is observed at the tyrosine residue of P3, and the glutamine or serine residue of P5.
(D) The divergent conformation of b-isox molecules
(E) Binding of b-isox to the β strand.

4. Discussion

Exceptional property of the b-isox molecules is revealed with theoretical modeling its crystal with the LC domain of

TLS. Our model demonstrates dynamic movement of growing process of the co-crystallization of the compounds and TLS. We describe these interactions of the LC domain of TLS to the growing crystal of b-isox.

Some LC domain-containing proteins have been identified as causative agents for neurodegenerative diseases, ALS and frontotemporal lobar degeneration [31, 32, 34]. Most of these proteins are RNA binding proteins and form insoluble aggregates that exert fatal effects on specific neuronal cells. It is a great concerning for the basic scientists and clinicians to uncover a trigger for stimulating formation of these aggregates. We suspect the small molecules like b-isox that we have been analyzing at this report to be a deleterious trigger. Therefore, our data here would present a valuable clue to development of the therapeutics for the neuronal disorders.

Specific binding motif of the LC domain of TLS works on formation of the co-crystallization. The LC domain of TLS contains a dozen of Y, Q, and S. Eleven of these amino acid sequences have a perfect match with the common motif: QS-X-YQ-X-QS (Fig.7A). These amino acid residues could bind the b-isox crystals through the β strand-like hydrogen bonds of the main chains, and the hydrogen bonds of the side chains. TLS molecules bind the b-isox crystals through multiple regions of these amino acids, and forms large complexes (Fig.7B).

Polypeptides without any specific structure are supposed to be suitable for binding to the b-isox crystals [35]. The LC domain of TLS does not have any specific structure [18, 36]. The polypeptide chains with specific structures like α helix and β sheet, have already had hydrogen bonds of the amide groups and the carbonyl groups of the main chains. These polypeptides are required to dissociate these hydrogen bonds in order to form the hydrogen bonds with b-isox. Therefore, the peptide without any structure, with no hydrogen bond, is favored to form a hydrogen bond with the strand of b-isox, suggesting that the LC domain of TLS fits well forming the β strand with b-isox.

Avidin is a biotin-binding protein biosynthesized in the oviducts of birds, and deposited in the whites of the eggs. The dissociation constant (Kd) of avidin is measured approximately at 10^{-15} M, making it one of the strongest known no-covalent bonds so far reported. The hydrogen bond between avidin and biotin is shown (Fig.7C). The bindings of Y33, threonine (T) 35, asparagine (N) 118 of the avidin side chains, to biotin molecules are similar to the bindings of the LC domain to b-isox. At the position P3, the binding of the side chain of tyrosine to the oxygen of biotin, are corresponded to one at the Y33. At the P5, bindings of the side chain of the glutamine and serine to the nitrogen of biotin are correspondent to the bindings of N118 and T35. These observations suggest that the bindings of Y, Q, and S to the biotin moiety of b-isox at the LC domain should resemble the binding of avidin to biotin. Prediction based on the consensus, QS-X-YQ-X-QS, presents QGYGQ, QGYGS, and SGYGA as high affinity sequence because P3 as Y and P5 as Q or S at the LC domain form avidin-like bindings.

B-isox molecules have a completely extended shape in solution, and their carbonyl groups and the amide groups align in the same orientation of the β strand. In theory, b-isox molecules form divergent conformations (Fig.7D), suggesting that b-isox forms the β strand structure only in the case of forming the crystal. This presents a hypothesis that addition of b-isox into cold solution induces small crystal formation and the LC domain is incorporated into the "seed of the crystal" growing up to large crystal.

Previous discussion presents a model depicting the co-crystallization of b-isox and the LC domains [20]. The LC domain with disordered random coiled structure could touch the groove of the crystal surface and form the β strand structure, incorporated into the growing crystal because the width of the groove of the crystal is supposed to be 9.4 Å, and this just fits the β strand of the polypeptide of the LC domain.

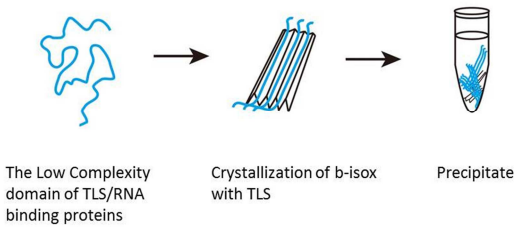

Figure 8. *Graphical Summary.*

The formation of the crystals and precipitations are depicted.

Just following the model presented by Kato et al., in the status of forming the β strand-like hydrogen bonds between the main chains of the β strands and the b-isox molecules, the distance between the main chains of the β strand and the lower layers is only 3 Å, touching the b-isox of the lower layer (Fig.7E) [20]. At this model, only the glycine residues are allowed for P1, P3, and P5 (magenta) of the polypeptide to slip into the groove of the b-isox crystal (Fig.7E). There is no sequence matched to "Gly-X-Gly-X-Gly" both in the LC domain of TLS and of TIA1. The hydrogen bond formation of the LC domains of TLS and TIA1 to b-isox requires space under the polypeptides for folding their side chains. Otherwise, no such interaction could occur. Taken together, the LC polypeptides are suggested to be incorporated into nascent growing surfaces and edges of the b-isox crystals instead of their binding the pre-assembled surface of the crystals (Fig.8).

In summary, the LC domain of TLS is preferable to form crystals with b-isox. The LC domain of the disordered structure could bind the b-isox crystal with the main and side chains, and also contains many Y, Q, and S, suggesting that it is suitable to form the co-crystal with b-isox. The LC domain is shown to be incorporated into the crystal during the process of the crystal growing.

5. Conclusion

The LC domain of TLS is proved to have potency to forming a crystal with the b-isox molecules. This is because the TLS-LC domain has disordered conformation, relatively many Y, Q, an S, and binds the b-isox crystal by the main and side chains. During elongation of the fine crystal of b-isox, the LC domain of TLS should be incorporated into the growing crystal of b-isox.

Acknowledgments

The authors would thank for excellent technical supports by Mr. Sei-ichi Aikawa and Fumiko Matsuzawa (Altif Laboratories Inc.), and also by Naomi Ueda. This study was supported by Grant-in-Aid for Scientific Research (B: nos22390057; 25293073). This work was also supported in part by a grant-in-aid for "Support Project of Strategic Research Center in Private Universities" from the Ministry of Education, Culture, Sports, Science and Technology (MEXT) to Saitama Medical University Research Center for Genomic Medicine.

References

[1] Kurokawa R (Ed.). Long Noncoding RNAs: Springer; 2015.

[2] Lipovich L, Tarca AL, Cai J, Jia H, Chugani HT, Sterner KN, Grossman LI, Uddin M, Hof PR, Sherwood CC, et al: Developmental changes in the transcriptome of human cerebral cortex tissue: long noncoding RNA transcripts. *Cereb Cortex* 2014, 24:1451-1459.

[3] Derrien T, Johnson R, Bussotti G, Tanzer A, Djebali S, Tilgner H, Guernec G, Martin D, Merkel A, Knowles DG, et al: The GENCODE v7 catalog of human long noncoding RNAs: analysis of their gene structure, evolution, and expression. *Genome research* 2012, 22:1775-1789.

[4] Carninci P, Kasukawa T, Katayama S, Gough J, Frith MC, Maeda N, Oyama R, Ravasi T, Lenhard B, Wells C, et al: The transcriptional landscape of the mammalian genome. *Science* 2005, 309:1559-1563.

[5] Khalil AM, Guttman M, Huarte M, Garber M, Raj A, Rivea Morales D, Thomas K, Presser A, Bernstein BE, van Oudenaarden A, et al: Many human large intergenic noncoding RNAs associate with chromatin-modifying complexes and affect gene expression. *Proc Natl Acad Sci U S A* 2009, 106:11667-11672.

[6] Djebali S, Davis CA, Merkel A, Dobin A, Lassmann T, Mortazavi A, Tanzer A, Lagarde J, Lin W, Schlesinger F, et al: Landscape of transcription in human cells. *Nature* 2012, 489:101-108.

[7] Necsulea A, Soumillon M, Warnefors M, Liechti A, Daish T, Zeller U, Baker JC, Grutzner F, Kaessmann H: The evolution of lncRNA repertoires and expression patterns in tetrapods. *Nature* 2014, 505:635-640.

[8] Chi KR: Finding function in mystery transcripts. *Nature* 2016, 529:423-425.

[9] Kurokawa R: Generation of Functional Long Noncoding RNA Through Transcription and Natural Selection. In *Regulatory RNAs.* Springer; 2012: 151-174

[10] Kurokawa R: Long noncoding RNA as a regulator for transcription. *Prog Mol Subcell Biol* 2011, 51:29-41.

[11] Kurokawa R: Promoter-associated long noncoding RNAs repress transcription through a RNA binding protein TLS. *Advances in experimental medicine and biology* 2011, 722:196-208.

[12] Kurokawa R: Initiation of Transcription Generates Divergence of Long Noncoding RNAs. In *Long Noncoding RNAs.* Springer; 2015: 69-91

[13] Kurokawa R, Rosenfeld MG, Glass CK: Transcriptional regulation through noncoding RNAs and epigenetic modifications. *RNA Biol* 2009, 6:233-236.

[14] Carninci P, Sandelin A, Lenhard B, Katayama S, Shimokawa K, Ponjavic J, Semple CA, Taylor MS, Engstrom PG, Frith MC, et al: Genome-wide analysis of mammalian promoter architecture and evolution. *Nat Genet* 2006, 38:626-635.

[15] Duret L, Chureau C, Samain S, Weissenbach J, Avner P: The Xist RNA gene evolved in eutherians by pseudogenization of a protein-coding gene. *Science* 2006, 312:1653-1655.

[16] Johnsson P, Ackley A, Vidarsdottir L, Lui W-O, Corcoran M, Grandér D, Morris KV: A pseudogene long noncoding RNA network regulates PTEN transcription and translation in human cells. *Nature structural & molecular biology* 2013, 20:440-446.

[17] Scarola M, Comisso E, Pascolo R, Chiaradia R, Maria Marion R, Schneider C, Blasco MA, Schoeftner S, Benetti R: Epigenetic silencing of Oct4 by a complex containing SUV39H1 and Oct4 pseudogene lncRNA. *Nat Commun* 2015, 6:7631.

[18] Yoneda R, Suzuki S, Mashima T, Kondo K, Nagata T, Katahira M, Kurokawa R: The binding specificity of Translocated in LipoSarcoma/FUsed in Sarcoma with lncRNA transcribed from the promoter region of cyclin D1. *Cell & bioscience* 2016, 6:4.

[19] Wang X, Arai S, Song X, Reichart D, Du K, Pascual G, Tempst P, Rosenfeld MG, Glass CK, Kurokawa R: Induced ncRNAs allosterically modify RNA-binding proteins in cis to inhibit transcription. *Nature* 2008, 454:126-130.

[20] Kato M, Han TW, Xie S, Shi K, Du X, Wu LC, Mirzaei H, Goldsmith EJ, Longgood J, Pei J, et al: Cell-free formation of RNA granules: low complexity sequence domains form dynamic fibers within hydrogels. *Cell* 2012, 149:753-767.

[21] Han TW, Kato M, Xie S, Wu LC, Mirzaei H, Pei J, Chen M, Xie Y, Allen J, Xiao G, McKnight SL: Cell-free formation of RNA granules: bound RNAs identify features and components of cellular assemblies. *Cell* 2012, 149:768-779.

[22] Lagier-Tourenne C, Cleveland DW: Rethinking ALS: the FUS about TDP-43. *Cell* 2009, 136:1001-1004.

[23] Kwiatkowski TJ, Jr., Bosco DA, Leclerc AL, Tamrazian E, Vanderburg CR, Russ C, Davis A, Gilchrist J, Kasarskis EJ, Munsat T, et al: Mutations in the FUS/TLS gene on chromosome 16 cause familial amyotrophic lateral sclerosis. *Science* 2009, 323:1205-1208.

[24] Vance C, Rogelj B, Hortobagyi T, De Vos KJ, Nishimura AL, Sreedharan J, Hu X, Smith B, Ruddy D, Wright P, et al: Mutations in FUS, an RNA processing protein, cause familial amyotrophic lateral sclerosis type 6. *Science* 2009, 323:1208-1211.

[25] Sun S, Ling S-C, Qiu J, Albuquerque CP, Zhou Y, Tokunaga S, Li H, Qiu H, Bui A, Yeo GW, et al: ALS-causative mutations in FUS/TLS confer gain and loss of function by altered association with SMN and U1-snRNP. *Nat Commun* 2015, 6.

[26] Lagier-Tourenne C, Polymenidou M, Cleveland DW: TDP-43 and FUS/TLS: emerging roles in RNA processing and neurodegeneration. *Hum Mol Genet* 2010, 19:R46-64.

[27] Sadek H, Hannack B, Choe E, Wang J, Latif S, Garry MG, Garry DJ, Longgood J, Frantz DE, Olson EN, et al: Cardiogenic small molecules that enhance myocardial repair by stem cells. *Proceedings of the National Academy of Sciences* 2008, 105:6063-6068.

[28] Song X, Wang X, Arai S, Kurokawa R: Promoter-associated noncoding RNA from the CCND1 promoter. *Methods in molecular biology* 2012, 809:609-622.

[29] Guex N, Peitsch MC: SWISS-MODEL and the Swiss-PdbViewer: an environment for comparative protein modeling. *Electrophoresis* 1997, 18:2714-2723.

[30] Rahman MM, Kitao S, Tsuji D, Suzuki K, Sakamoto J-I, Matsuoka K, Matsuzawa F, Aikawa S-I, Itoh K: Inhibitory effects and specificity of synthetic sialyldendrimers toward recombinant human cytosolic sialidase 2 (NEU2). *Glycobiology* 2013, 23:495-504.

[31] King OD, Gitler AD, Shorter J: The tip of the iceberg: RNA-binding proteins with prion-like domains in neurodegenerative disease. *Brain Research* 2012, 1462:61-80.

[32] Alberti S, Halfmann R, King O, Kapila A, Lindquist S: A systematic survey identifies prions and illuminates sequence features of prionogenic proteins. *Cell* 2009, 137:146-158.

[33] Livnah O, Bayer EA, Wilchek M, Sussman JL: Three-dimensional structures of avidin and the avidin-biotin complex. *Proceedings of the National Academy of Sciences of the United States of America* 1993, 90:5076-5080.

[34] Kim HJ, Kim NC, Wang YD, Scarborough EA, Moore J, Diaz Z, MacLea KS, Freibaum B, Li S, Molliex A, et al: Mutations in prion-like domains in hnRNPA2B1 and hnRNPA1 cause multisystem proteinopathy and ALS. *Nature* 2013, 495:467-473.

[35] Berchowitz Luke E, Kabachinski G, Walker Margaret R, Carlile Thomas M, Gilbert Wendy V, Schwartz Thomas U, Amon A: Regulated Formation of an Amyloid-like Translational Repressor Governs Gametogenesis. *Cell* 2015, 163:406-418.

[36] Schwartz Jacob C, Wang X, Podell Elaine R, Cech Thomas R: RNA Seeds Higher-Order Assembly of FUS Protein. *Cell Reports* 2013, 5:918-925.